International Journal of GEOMATE, Feb., 2019 Vol.16, Issue 54, pp.158 - 163
Geotec., Const. Mat. & Env., DOI: https://doi.org/10.21660/2019.54.8315
ISSN: 2186-2982 (Print), 2186-2990 (Online), Japan

MULTI-CHANNEL FIBRE BRAGG GRATING SENSORS FOR UNIAXIAL COMPRESSION TEST ON LIMESTONE ELASTICITY BEHAVIOUR

*Balarabe Wada Isah[1], Hisham Mohamad[2], and Niraku Rosmawati Ahmad[3]

[1,2,3] Civil & Environmental Engineering Department, Universiti Teknologi PETRONAS, Malaysia

*Corresponding Author, Received: 01 Oct. 2018, Revised: 04 Dec. 2018, Accepted: 25 Dec. 2018

ABSTRACT: In rock mechanics, measurement of small strain response is the most basic and significant means of assessing rock mechanical and elasticity behavior. To overcome the difficulties of mounting, handling many cables, dependency of the stain responds measured to the properties of the sensor components, this paper intends to explore the applicability of a novel multi-channel Fiber Bragg Grating sensors (MC-FBGs) for determining small strain response of cylindrical rock specimen under uniaxial compression test for assessing deformability properties. The concept, design and embedment technique of MC-FBGs employed in the experiment are illustrated concisely. To analyze the stress-strain respond of a cylindrical limestone specimen, two axial FBGs placed diametrically opposite to each other along the longitudinal axis of the specimen and two radial FBGs embedded opposite to each other circumferentially within the central one-third portion of the specimen were adopted for axial and radial strain response measurement. In addition, two electrical resistance-based strain gauges (SG), one mounted axially and the other attached radially along the circumference, are used for comparative measurements with the FBGs. The values of unconfined compressive strength, Young's modulus, crack initiation and crack damage stress obtained from MC-FBGs and SG are in good agreement. It could be deduced that MC-FBGs can measure small strain response of limestone, stiffness anisotropy as well as measure the vital stages of rock failure mechanisms proficiently. MC-FBGs could serve as an alternative approach for determining reliable, accurate and precise compressive strain response of a limestone.

Keywords: Multichannel FBG sensor, Uniaxial compression test, Strain Response, Limestone

1. INTRODUCTION

The study of mechanical behaviour of rocks under the influence of external loading is very vital as it set a platform for understanding various natural geophysical processes that occurred in earth's crust, also to provide engineering solutions associated with the wide range of human activities especially with the evolvement of large geotechnical engineering structures such as deep tunnels, boreholes for oil and gas and tunnel for storage of radioactive waste. Strain response plays an important role in analyzing the mechanical behavior of rocks either in the small-scale specimen or large-scale geotechnical structures, especially for structural health assessment. Most rocks are very stiff, therefore their strain response to loading is very small (microstrain) [1]. This requires a very accurate and high precision device to obtain a realistic stress-strain relationship of the rocks.

In the laboratory, uniaxial compression test (UCT) is one of the basic and vital tests routinely performed on rock specimens[2]. It is imperative to highlight that UCT is methodized by both the International Society for Rock Mechanics (ISRM) and the American Society for Testing and Materials (ASTM). Varieties of instruments and devices are coopted during the UCT test to characterize the small strain response of rocks with reasonable accuracy. Over the years, various devices were implemented to measure strain in UCT of rocks; Linear variable differential transducers (LVDT) [3], strain gauges (SG) [4], acoustic emission (AE) [5], digital image correlation (DIC) [6], extensometer [7], and digital terrestrial photogrammetry [8]. Despite the fact that the existing strain monitoring techniques are comparatively considered precise and reliable throughout the measuring period, the inherent limitations or deficiencies of non-immune to electrical short-circuiting, effect of lightning, electromagnetic interference (EMI), difficulties in mounting, signal loss over long range experience by some of the techniques, use of many cables and post-experimental calculations steal continued to exist [9]. Moreover, the measured strain from the conventional strain devises is heavily dependent on the properties of the device components, defective component leads to uncertainty in results. Which is why many other new techniques have continued to evolve.

MC-FBGs have continued to gain more attraction due to its diversity in the measurement of quantities (e.g.; strain, temperature, pressure, force, displacement, vibration etc) [10]. The versatility of

MC-FBGs is due to magnificent advantages of being; light in weight, small in size, single and multi-point sensing, resistance to hash laboratory environmental condition, multifunctioning, linear output, resistance to corrosion, immune to electrical short-circuiting, the effect of lightning and EMI [11]. FBGs have demonstrated a wide range of application in, security, pipelines, wells, seismic, and for smart structures in civil engineering [12–17].

Nevertheless, it is useful to mention some of the disadvantages of using FBGs; limited suppliers and a lack of standards. FBGs provide a point or quasi-distributed sensing measurements. Where distributed measurement is required, distributed fiber optics sensors based on Brillouin Optical Time Domain Analysis (BOTDA) or Brillioun Optical Time Domain Reflectometry (BOTDR) are most suitable [18,19].

Over the years, FBG sensor has gained acceptance for use in determining the mechanical behavior of rocks[11], [20–22].

In this paper, a new method of measuring strain response on limestone specimen using multi-channel FBGs is initiated and implemented on brittle rock (limestone) to capture the axial and radial strain response of a cylindrical core specimen. By equating the measured values obtained from FBGs with that of the SG, the practicability and efficiency of the FBGs arrangement are asserted.

2. WORKING PRINCIPLE OF MULTICHANNEL FBG SENSOR

Basically, there are two types of optical fibers: multi-mode optical fiber (MMOF) and single mode optical fiber (SMOF). MMOF has a relatively large core that transmits multiple rays or mode of light. It is suitable for short distance signal transmission. On the other hand, SMOF is designed to transmit a single ray or mode of light as a carrier, it is used for transmitting signals over a long distance. SMOF is suitable for a wide range of application with wavelength capability between 488 nm to 1625 nm. The fiber core can be either Germania doped fiber or pure silica. The Germania doped substantially improve photosensitivity making it an ideal candidate for FBGs fabrication. Pure silica option improves hydrogen resistance of SMOF making it suitable for high-temperature applications such as in oil and gas wells with minimal photodarkening. FBGs is a distributed Bragg reflector embossed within a small section of a single mode optical fiber SMOF which can reflect a specific wavelength of light and transmits all the other wavelengths.

FBGs are formed by engraving an unseen permanent periodic refractive index change in SMOF core. The components of SMOF are cladding and core, the refractive index of the core (inner part) is greater than that of the cladding (surrounding) which ensure total internal reflection. Schematic diagram of the FBGs working principle is shown in Fig. 1. External factors such as heat and pressure will cause a shift in the wavelength of the reflected light; this variation can then be translated into physical engineering units such as amplitude, strain, and temperature with the help of interrogator. Certain interrogators available in the market can detect a shift in the Bragg wavelength of as small as 1pico meter (10^{-12} m). From Fig. 1, the reflected light's wavelength can be obtained using Eq. (1) [23].

$$\lambda_B = 2n_{eff}\Lambda \quad (1)$$

Where; n_{eff} is the refraction index of the fibre core and Λ is the grating period of index modulation. Shift in the wavelength ($\Delta\lambda_B$) during the experiment can be determined using Eg. (2) [24].

$$\Delta\lambda_B = \lambda_B(1 - p_e)\Delta\varepsilon + (\alpha + \xi)\Delta T \quad (2)$$

Where; p_e is an effective photo-elastic constant of the fiber core material, $\Delta\varepsilon$ is change in the strain, ξ and α are temperature coefficients, and ΔT is change in temperature.

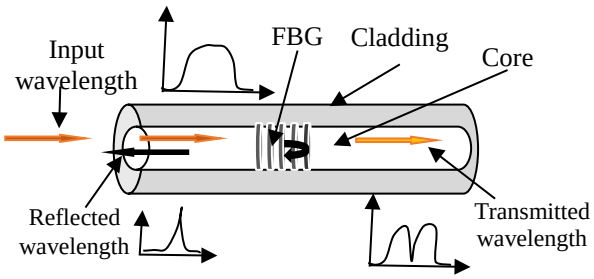

Fig.1 Schematic diagram of FBG working principle

When the temperature is constant, Eq. (2) can be written as Eq. (3):

$$\Delta\lambda_B = \lambda_B\, k\, \varepsilon \quad (3)$$

Where k is a strain constant $\cong 0.78$ for an ordinary bare SMOF. The entire compression test experiment was conducted in a relatively short period of time, therefore thermal variation within the vicinity of the gratings is neglected.

2.1 Design of Multichannel FBGs

The whole experiment was conducted using standard SMOF (SMF-28e) to eradicate

attenuations resulting from transmission medium or bending. Two MC-FBGs having two gratings inscribed in one SMOF were formed. Each grating is assigned a different Bragg wavelength (λ_B) which enable the interrogator to record readings from various gratings at the same time using wavelength division multiplexing (WDM) program. Various wavelengths assigned are within the range of 1528 nm-1560 nm making sure that each sensor works within a distinctive spectral range. Table 1 depicted the specifications of the four FBG sensors deployed, marked as V1, V2, L1 and L2

With the aid of epoxy resin adhesive, FBGs are embedded into the limestone. Limestone surface was furnished using sandpaper, FBGs are bonded and the bonding cured for 24 hours.

Table 1 Detail specifications of the FBG sensors utilized

Parts	V1	V2	L1	L2
$\boldsymbol{\lambda_B}$ $(\boldsymbol{nm})$	1560.1	1545.5	1535.1	1538.5
L (mm)	20	20	20	20
FWHM $\pm \mathbf{0.1}$ (nm)	0.3	0.3	0.3	0.3
BW@3dB (nm)	0.168	0.157	0.138	0.151
SLSR (dB)	16	16	17	20
Reflectivity (%)	90	90	90	90

L: Length of the gratings

$\boldsymbol{\lambda_B}$: Central wavelength (CW) corresponding to each grating

SLSR (Side Lobe Suppression Ratio): Highest secondary peak bigger than 3 dB amplitude within +/- 3 nm from CW. For Standard FBGs SLSR > 15 dB

FWHM (Full Width at Half Maximum): FBGs width at 50% (-3 dB) from FBGs maximum Reflectivity, measured from Reflection Spectra

Reflectivity R% = 1-10 (T(dB)/10): Measured from transmission spectra

3. EXPERIMENTAL SETUP

3.1 Specimen Preparation

A 50-mm diameter limestone rock core obtained from tunneling site in Ipoh, Perak, Peninsular Malaysia was used in the study. The rock core was cut into the laboratory testing specimen's size using aspect ratio (ratio of length to diameter) of 2.0 at thin-section laboratory. The two faces are trimmed making sure that a perfect right circular cylinder is obtained in accordance with ISRM standard. Prior to the testing, the specimen is oven dried for 24 hours to ensure testing on the dry state. Table 2 summarises the properties of the specimen.

In this experiment, the limestone surface was polished using sandpaper, and the adhesive was applied onto the FBGs in accordance to the measurement position with the help of sellotape.

Table 2 Properties of the limestone specimens

Height (cm)	Dia. (cm)	Weight (g)	Vol. (mm^3)	Density (g/cm^3)
9.995	4.992	570.1	195.7	2.913

3.1.1 Apparatus

The test is conducted using the RT-1000 testing machine manufactured by IPC global rock tester with an axial loading capacity of 1000 kN. A single desktop computer with the software of the machine installed is fully dedicated to the machine. The software provides the user with several options including the type of test (dynamic or static) and the loading condition (axial force-controlled, or displacement-controlled mode). Limestone core (instrumented with strain SG and FBGs positioned along an axial and radial direction to record axial (ε_a) and radial (ε_r) strain respectively) is placed on the lower plate of the machine (Fig. 2). For better comparison of the recorded data, the SG and the FBGs are positioned adjacent to each other respectively (Fig. 3). The test was carried out using displacement-controlled rate of 0.5 mm/s.

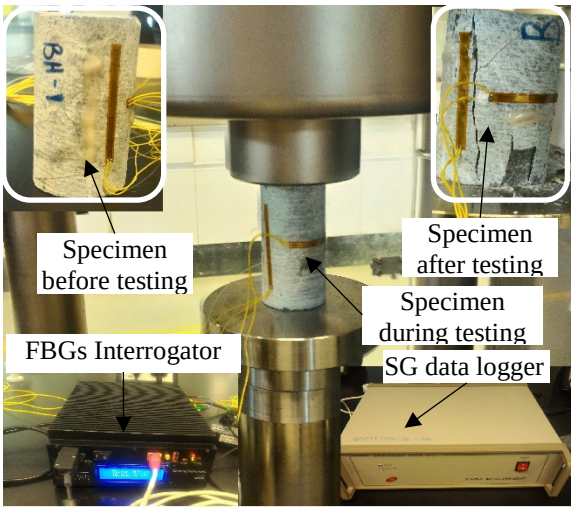

Fig. 2 Pictorial view of experimental apparatus and testing procedure

4. RESULTS AND DISCUSSION

This section introduces the outcome of the compression test conducted on limestone core in

IPC global rock tester machine using MC-FBGs and SG.

The entire experiment was performed at relatively room temperature to prevent the effect of temperature variations on FBGs. The axial force recorded during the test is divided by the initial cross-sectional area of the specimen to obtain the axial stress. The stress plotted against the axial and radial strain responses recorded by FBGs and SG, is presented in Fig. 4 with each response indicated with a distinct color. The strain response portrait by FBGs ($\boldsymbol{\varepsilon_a}$ **– FBG and** $\boldsymbol{\varepsilon_r}$ -FBG) signifies the average strain accorded by the two axial (V1 and V2) and two radial (L1 and L2) FBGs respectively. $\boldsymbol{\varepsilon_r}$-SG and $\boldsymbol{\varepsilon_a}$-SG represent the radial and axial strain by SG while $\boldsymbol{\varepsilon_v}$-FBG and $\boldsymbol{\varepsilon_v}$-SG denotes the volumetric strain by FBGs and SG respectively. The results of the compression test indicated that the strain response recorded by FBGs and SG are in good agreement. The strain measured by the FBGs and SG are almost similar.

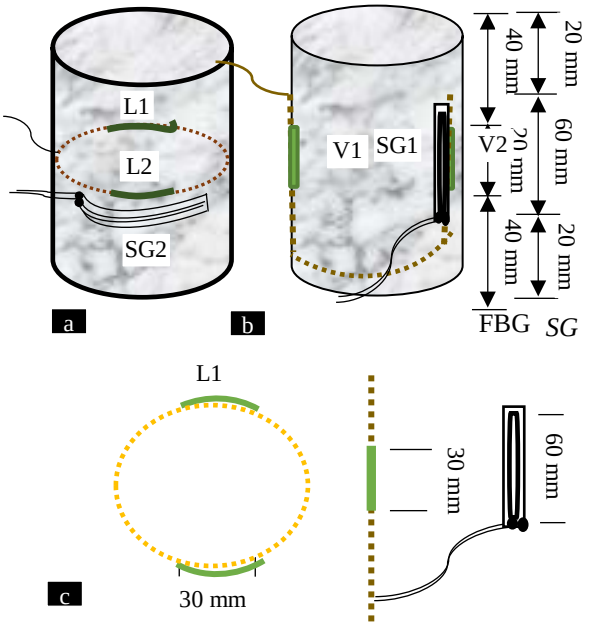

Fig. 3 Schematic view of sensors layout and embedment on limestone: (a) Radial layout of FBGs and SG (b) Axial layout of FBGs and SG (c) Dimension and radial positioning of the sensors

The failure pattern of the limestone core tested is vertical splitting [25]. Figure 4 explains the existing crack closure scenario in the specimen. Subsequently, FBGs was able to locate widely accepted four-stage model of rock failure mechanism: crack closure (σ_{cc}), crack initiation stress (σ_{ci}), crack damage stress (σ_{cd}) and uniaxial strength (UCS) which are very important parameters in the analysis of limestone behavior. Also, elastic parameters (Young's modulus E and poison's ratio) which provides essential information needed for the design of excavation, borehole stability and defining parameters needed for constitutive models (Table 3) are determined. While E and poison's ratio informed about the mechanical behavior of the rocks, $\sigma_{ci,\text{ and }}\sigma_{cd}$ are thresholds that serve as warning indicators of rock mass damage and breakout respectively. Beyond $\sigma_{cd,}$ crack propagation can no longer be controlled resulting in an unstable process.

Comparatively, values obtained by FBGs and SG are in close agreement (Table 3). Even though both sensors provide reliable information, FBGs have shown promising performance. Therefore FBG can reliably measure the strain response and potential crack grows of a limestone core specimen effectively. Moreover, reliable, accurate and high precision data of rock deformation are extremely useful and valuable to provide raw data and theoretical mechanism needful for further experimental analysis, numerical simulation and field applications. While FBGs can be most suitable for use in certain difficult areas, a huge gap exists in the field especially with the evolvement of large underground tunnel constructions, particularly around Ipoh area where limestone is the predominant types of rock. FBGs application in the laboratory UCT is fundamental for more complex test and field monitoring application.

Table 3. Estimated parameters from the test

Variables	FBGs	SG
σ_{cd} (MPa)	54	53
σ_{ci} (MPa)	39	40
E (GPa)	37.812	40.7
Poison's Ratio	0.236	0.26
UCT (MPa)	58	58

5. CONCLUSION

Smart way of measuring strain response of limestone rock significantly with high precision using a new MC-FBGs, under uniaxial compression for on-specimen measurement is presented. The advantages offered by FBG sensing techniques coupled with the need for an alternate simple and accurate technique to breach the shortcomings of the existing are the stimuli for this study.

MC-FBG is shown to be effective in monitoring the strain responses of limestone core specimen subjected to UCT with ease high resolution and accuracy. It was found out that the results recorded by FBGs resemble those obtained by SG.

The experiment reported is an effort and try-out on the use of FBGs to measure the strain responses

of limestone core specimen under UCT not considering the influence of temperature. Further investigation may incorporate the influence of temperature on FBG and more complex laboratory experiments on sedimentary rock cores.

6. ACKNOWLEDGMENTS

The authors are grateful to Universiti Teknologi PETRONAS (UTP) for the financial support given through the graduate assistantship (GA) scheme.

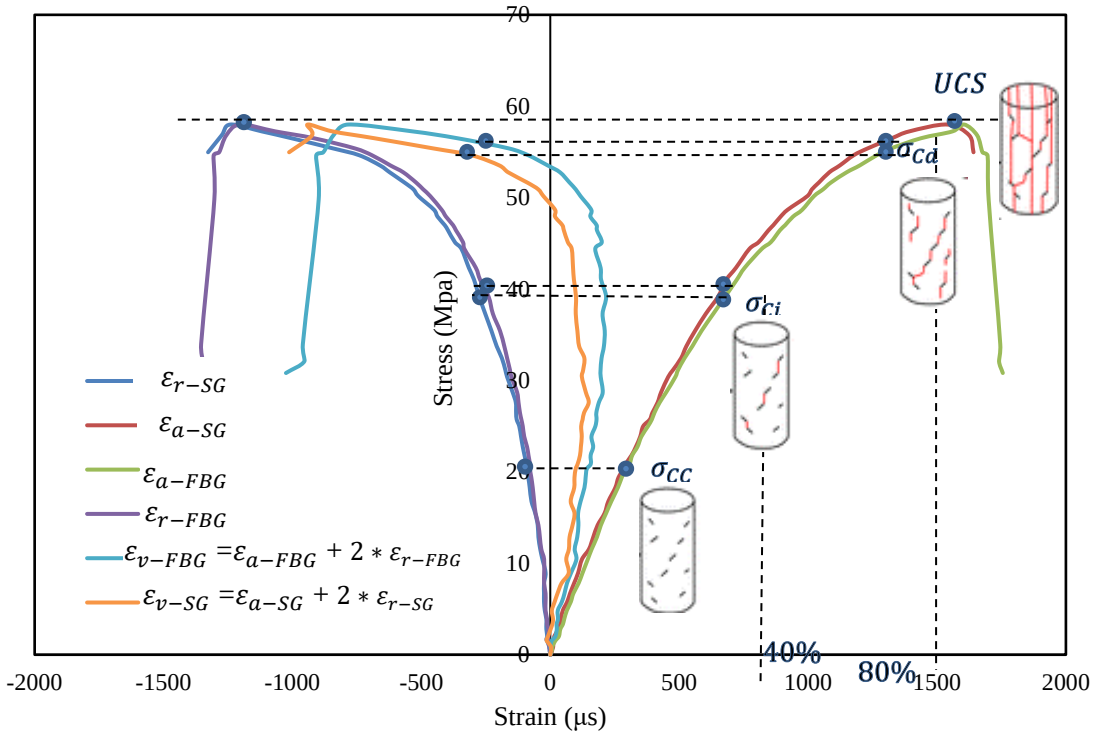

Fig 5. Stress-strain curve of limestone specimen under uniaxial compression test

5. REFERENCES

[1] Hamdi P., Characterization of Brittle Damage in Rock from the Micro to Macro Scale. Simon Fraser University, 2008.

[2] Roshan H., H. Masoumi, and P. Hagan, "On size dependent uniaxial compressive strength of sedimentary rocks in reservoir geomechanics," in 50th US Rock Mechanics/Geomechanics Symposium, ARMA, Vol. 3, 2016 pp: 2322 – 2327.

[3] Bartmann K. and M. Alber, "Experimental Determination of Crack Initiation and Crack Damage of Two Granites," Procedia Engineering, Vol. 191. 2017, pp. 119–126.

[4] Roshan H., H. Masoumi, and K. Regenauer-Lieb, "Frictional behavior of sandstone: A sample-size dependent triaxial investigation," J. Struct. Geol., Vol. 94, 2017, pp. 154–165.

[5] Hoek E. and C. D. Martin, "Fracture initiation and propagation in intact rock–a review," J. Rock Mech. Geotech. Eng., Vol. 6, No. 4, 2014, pp. 287–300.

[6] Munoz H., A. Taheri, and E. K. Chanda, "Pre-Peak and Post-Peak Rock Strain Characteristics During Uniaxial Compression by 3D Digital Image Correlation," Rock Mech. Rock Eng., Vol. 49, No. 7, 2016, pp. 2541–2554.

[7] Munoz H. and A. Taheri, "Specimen aspect ratio and progressive field strain development of sandstone under uniaxial compression by three-dimensional digital image correlation," J. Rock Mech. Geotech. Eng., Vol. 9, No. 4, 2017, pp. 599–610.

[8] Firpo G., R. Salvini, M. Francioni, and P. G. Ranjith, "Use of Digital Terrestrial Photogrammetry in rocky slope stability analysis by Distinct Elements Numerical Methods," Int. J. Rock Mech. Min. Sci., vol. 48, No. 7, 2011, pp. 1045–1054.

[9] Isah B. W., H. Mohamad, and I. S. H. Harahap, "Measurement of small-strain stiffness of soil in a triaxial setup : Review of local instrumentation," Int. J. Adv. Appl. Sci., Vol. 5, No. 7, 2018, pp. 15–26.

[10] Sun Y., Q. Li, and C. Fan, "Laboratory core flooding experiments in reservoir sandstone under different sequestration pressures using multichannel fiber Bragg grating sensor arrays,"

Int. J. Green. Gas Control, Vol. 60, 2017, pp. 186–198.

[11] Park J., Y. S. Kwon, M. O. Ko, and M. Y. Jeon, "Dynamic fiber Bragg grating strain sensor interrogation with real-time measurement," Opt. Fiber Technol., Vol. 38, 2017, pp. 147–153.

[12] Hong C. Y., Y. F. Zhang, M. X. Zhang, L. M. G. Leung, and L. Q. Liu, "Application of FBG sensors for geotechnical health monitoring, a review of sensor design, implementation methods and packaging techniques," Sensors Actuators, A Phys., Vol. 244, 2016, pp. 184–197.

[13] Bin Huang A., C. C. Wang, J. T. Lee, and Y. Te Ho, "Applications of FBG-based sensors to ground stability monitoring," J. Rock Mech. Geotech. Eng., Vol. 8, No. 4, 2016, pp. 513–520.

[14] Kahandawa G . C., J. Epaarachchi, H. Wang, and K. T. Lau, "Use of FBG sensors for SHM in aerospace structures," Photonic Sensors, Vol. 2, Vo. 3, 2012, pp. 203–214.

[15] Koyama S., A. Sakaguchi, H. Ishizawa, and K. Yasue, "Vital Sign Measurement Using Covered FBG Sensor Embedded into Knitted Fabric for Smart Textile," J. Fiber Sci. Technol., Vol. 73, No. 11, 2017, pp. 300–308.

[16] Lee C. C., K. Hung, W.-M. Chan, Y. K. Wu, S.-O. Choy, and P. Kwok, "FBG sensor for physiologic monitoring in M-health application," in SPIES-OSA-IEEE, Vol. 8311, 2011, p. 83111S.

[17] Wang J.Y., T.-Y. Liu, C. Wang, X.-H. Liu, D.-H. Huo, and J. Chang, "A micro-seismic fiber Bragg grating (FBG) sensor system based on a distributed feedback laser," Meas. Sci. Technol., Vol. 21, No. 9, 2010, p. 094012.

[18] Mohamad H., P. J. Bennett, K. Soga, R. J. Mair, C.H. Lim, *et. al.* "Monitoring Tunnel Deformation Indued by Closed-Proximity Bored Tunneling Using Distributed Optical Fiber Strain Measurements," Geotechnical Special Publication (175) 7th FMGM 2007, no. pp. 1–12, 2007.

[19] Mohamad H., and B. P. Tee, "Instrumented pile load testing with distributed optical fibre strain sensor," Jurnal Teknologi, vol. 77, no. 11, pp. 1-7, 201.

[20] Castro-Caicedo A., M. J. Nieto-Callejas, and P. Torres, "Fiber Bragg grating strain sensor for hard rocks," no. September, 2015, p. 963449.

[21] Schmidt-Hattenberger C., M. Naumann, and G. Borm, "Fiber Bragg grating strain measurements in comparison with additional techniques for rock mechanical testing," IEEE Sens. J., Vol. 3, No. 1, 2003, pp. 50–55.

[22] Zhao Y., N. Zhang, and G. Si, "A fiber bragg grating-based monitoring system for roof safety control in underground coal mining," Sensors (Switzerland), Vol. 16, 2016, pp 1-13.

[23] Morey W., G. Meltz, H. Glenn, and W. Glenn, "Fiber optic Bragg grating sensors," Proc. SPIE Fiber Opt. Laser Sensors VII, Vol. 1169, 1989, pp. 98–107.

[24] Hill K. O. and G. Meltz, "Fiber Bragg Grating Technology Fundamentals and Overview," IEEE J. Light. Technol., Vol. 15, No. 8, 1997, pp. 1263–1276.

[25] Hazzard J. F., R. P. Young, and S. C. Maxwell, "Micromechanical modeling of cracking and failure in brittle rocks," J. Geophys. Res. Solid Earth, vol. 105, no. B7, pp. 16683–16697, 2000.

Copyright © Int. J. of GEOMATE. All rights reserved, including the making of copies unless permission is obtained from the copyright proprietors.